

Characterization of Supported Vanadium Oxide Catalysts. Nature of the Vanadium Species in Reduced Catalysts

P. Concepción,[†] H. Knözinger,[‡] J. M. López Nieto,^{*,†} and A. Martínez-Arias[§]

Instituto de Tecnología Química, Universidad Politécnica de Valencia, UPV-CSIC, Avda. Los Naranjos s/n, 46022 Valencia, Spain, Institut für Physikalische Chemie, Universität München, Butenandtstrasse, 5–13 (Haus E), 81377 München, Germany, and Instituto de Catálisis y Petroleoquímica, CSIC-UAM, Cantoblanco, 28049 Madrid, Spain

Received: March 9, 2001; In Final Form: November 6, 2001

The nature and redox properties of vanadium species on metal oxide supported vanadium catalysts have been studied. The calcined metal oxides—Al₂O₃, MgO, Mg–Al–hydrotalcite (Al/Mg = 0.33), and Mg–Al–Spinel (Al/Mg = 3.0)—have been employed as supports. TPR and IR spectra of adsorbed CO show a different reducibility of the vanadium species related to the acid–base character of the metal oxide support. This is also confirmed by the EPR results of both calcined and reduced catalysts. A reduction of V⁵⁺ to the V³⁺ species seems to be more favored on acid metal oxides. On basic metal oxide supports, the reducibility seems to be hindered, leading preferentially to the formation of V⁴⁺, although V³⁺ ions are also formed at higher reduction temperatures. A shift in the carbonyl frequency of the V⁴⁺–CO and V³⁺–CO complexes to lower frequencies by increasing the basicity of the support could be related to an electron donor effect of the support on the electron density of the vanadium species. In addition, a higher reoxidation ability of the V⁴⁺ and V³⁺ species is observed on the more acidic supports than on the basic ones.

1. Introduction

Supported vanadium oxides are known to be selective catalysts in a number of catalytic reactions, i.e., oxidation of methanol, methane, and olefins; oxidation and ammoxidation of aromatic hydrocarbons; and the selective catalytic reduction of NO_x.^{1–5} Recently, they have been proposed as selective catalysts in the oxydehydrogenation (OXDH) of short chain paraffins,^{1–3,6–10} although their catalytic properties depend on both the V loading and the acid–base nature of the oxide support.

It is generally accepted that the acid–base nature of the metal oxide support strongly influences both the nature and distribution of vanadium species.^{1–6,11,12} The different catalytic properties of bulk and supported vanadia catalysts can usually be related to modifications in the coordination and environment of the V species, which can modify its redox properties.

Because both redox and acid–base properties appear to be important in these catalysts, it is interesting to study supported vanadium oxide catalysts by infrared spectroscopy of adsorbed CO because this methodology provides additional information on the nature of acid and reduced sites. IR spectroscopy of adsorbed CO as a probe molecule has been extensively used for characterization of Lewis acid sites on catalyst surfaces.^{13–19} Heats of adsorption of CO on oxides are usually low, and low temperatures are therefore required for IR adsorption studies. However, the weak interaction energies make CO a reasonably selective probe molecule for the characterization of surface coordination sites. If π back-donation does not contribute to the coordination bond, purely electrostatic models can be used

to describe the adsorption interaction of CO with a cationic surface site. Consequently, several attempts have been made to correlate carbonyl frequency shifts with the electric field strength produced by the surface cation.^{20–23} However, in the case of metal ions having significant d-electron density (such as V³⁺ ions) π back-bonding is expected, and in this case, purely electrostatic models are not valid. Because of the high covalent character of the metal–oxygen bond in most transition metal oxides, the first and second coordination spheres may affect the electron-acceptor properties of the central metal ion. Therefore, metal ions with the same coordination number can differ strongly in their electrophilic properties depending on the nature and the coordination state of the ligands.²⁴ At the moment, only a few studies on the adsorption of CO on V-containing catalysts have been reported.^{25–32} The reported data demonstrated that bands observed in the 2212–2180 cm^{−1} region were easily removed by evacuation. These bands were attributed to V⁴⁺–CO carbonyls.^{25–29} In contrast, bands below 2192 cm^{−1}, could hardly be eliminated by evacuation. These bands were explained by the participation of back π bonding in V³⁺–CO carbonyls.^{25,28,30,33–36} V⁵⁺ ions do not form stable complexes with CO even at low temperature.^{25,27,32} It is therefore proposed that combining redox cycles and infrared spectra of adsorbed CO would provide information on the nature of reduced vanadium species in selective oxidation catalysts.

The aim of the present paper is to correlate the reducibility and nature of the reduced vanadium species with the acid–base character of the support. As the structure of the vanadium–oxygen species determines the reducibility of the vanadium cations, materials in which the vanadium species are well dispersed on the support in tetrahedral coordination are used. These catalysts have been proposed as active and selective in the OXDH of short chain alkanes.^{1,6,7}

* To whom correspondence should be addressed. E-mail: jmlopez@itq.upv.es.

[†] Universidad Politécnica de Valencia.

[‡] Universität München.

[§] Instituto de Catálisis y Petroleoquímica.

TABLE 1: Characteristics of Supported Vanadium Oxide Catalysts

catalyst	S_{BET} ($\text{m}^2 \text{g}^{-1}$)	V content (wt % V_2O_5)	θ^a	TPR- H_2		
				T onset (K)	T max (K)	H_2 uptake ^b
$\text{VO}_x/\text{Al}_2\text{O}_3$	160	7.0	0.3	573	738	1.10
VO_x/SP	210	20.1	0.6	673	813	0.63
VO_x/HT	166	37.3	1.5	694	858	0.46
VMgO	108	20.1	1.2	723	841	0.65

^a Vanadium superficial coverages, θ , have been obtained assuming the theoretical monolayer of vanadium to be 4.98×10^{14} molecules $\text{V}_2\text{O}_5 \text{ cm}^{-2}$ (ref 1). ^b H_2 uptake expressed as mol of H_2 per mol of V atom.

2. Experimental Section

2.1. Catalyst Preparation. Commercial $\gamma\text{-Al}_2\text{O}_3$ (Girdler T126), synthesized MgO, and heat-treated Mg–Al mixed oxides with hydrocalcite and spinel structures have been used as supports and referred to as Al_2O_3 , MgO, HT, and SP, respectively. MgO was obtained from magnesium oxalate by calcination in air at 973 K for 3 h.³⁷ Mg–Al–O mixed oxides with hydrocalcite and spinel structures were obtained by continuous coprecipitation from aqueous solutions of magnesium and aluminum nitrates with theoretical Al/Mg atomic ratios of 0.33 and 3.0, respectively, at a constant pH of 13 and at room temperature.³⁸ In both cases, the gel obtained was aged at 333 K for 18 h and then filtered and washed until a pH of 7 was obtained. The solids were then dried at 373 K overnight and calcined in air at 723 K for 18 h.

Supported vanadium catalysts were prepared by impregnation of the oxide support with ammonium metavanadate aqueous solutions, according to the preparation procedure reported previously.^{6,7} Then, the solids were filtered and dried at 353 K for 16 h. All samples were calcined at 873 K for 4 h. The characteristics of the catalysts are summarized in Table 1.

2.2. Catalyst Characterization. Temperature programmed reduction (TPR) results were obtained in a Micromeritics apparatus. Samples of 100 mg were first treated in argon at 673 K for 1 h, cooled to room temperature, and subsequently contacted with an H_2/Ar mixture (molar ratio of 0.15 and a total flow of 3 L h^{-1}). The samples were heated, at a rate of 10 K min^{-1} , to a final temperature of 1273 K.

IR spectroscopy studies were carried out with a Bruker IFS-66 FT spectrometer at a spectral resolution of 1 cm^{-1} and accumulations of 128 scans. Self-supporting wafers (ca. 10 mg cm^{-2}) were prepared from the sample powders and heated directly in the IR cell. Prior to the measurements, all samples were activated for 1 h in a flow of oxygen at 773 K followed by 1 h evacuation (10^{-3} Pa; 1 hPa = 1 mbar) at the same temperature. To study the nature of V species during the TPR experiments, the samples were reduced for 1 h in a flow of hydrogen at 773 and 873 K followed by evacuation (10^{-3} Pa) for another hour at the same temperature, respectively. After the self-supporting wafers were cooled to 85 K in a vacuum, CO was adsorbed at an equilibrium pressure of 20 hPa. The elimination of adsorbed CO was done by evacuation of the IR cell at different times. A purpose made transmission IR cell allowed the IR measurements to be performed at temperatures between 85 K (LT) and room temperature (RT).³⁹

Electron paramagnetic resonance spectra (EPR) were recorded at 77 K on a Bruker ER-200 spectrometer working in the X band and calibrated with a DPPH standard ($g = 2.0036$). Quantitative analysis was carried out by double integration of the EPR spectra and comparison with a copper sulfate ($\text{CuSO}_4 \cdot$

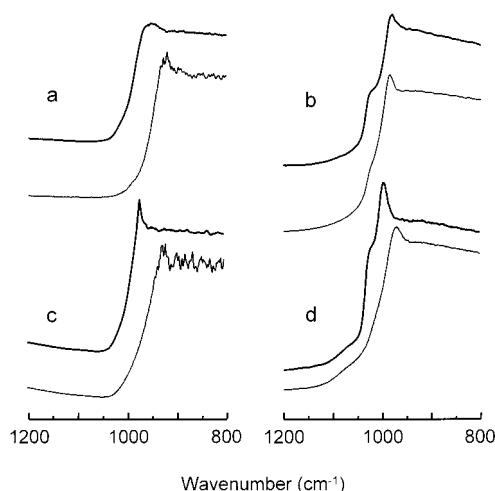


Figure 1. FTIR spectra in the low-frequency region of calcined samples (—) and samples reduced at 873 K (---): (a) VMgO, (b) $\text{VO}_x/\text{Al}_2\text{O}_3$, (c) VO_x/HT , and (d) VO_x/SP samples.

$5\text{H}_2\text{O}$) standard. Portions of ca. 30 mg of sample were introduced into an EPR quartz probe cell and handled in a conventional high vacuum line for the different treatments. In all cases, the samples were extensively outgassed at room temperature prior to recording spectra. The samples were always pretreated in 300 hPa of oxygen at 773 K (calcined sample). Reduction treatments were performed by heating for 1 h in 100–200 hPa of H_2 at the corresponding temperature (T_r), followed by outgassing for 0.5 h at the same temperature.

3. Results and Discussion

The characteristics of supported vanadia catalysts are shown in Table 1. The vanadium content in these samples has been varied in order to obtain tetrahedral V^{5+} species. These samples are active and selective in the OXDH of short chain alkanes although their catalytic behavior strongly depends on the metal oxide support and the alkane fed.^{6,7}

3.1. Temperature-Programmed Reduction. The TPR profiles exhibit only one prominent maximum. The onset temperature, T_{onset} , and the maximum hydrogen consumption, T_{max} , as well as the hydrogen consumption are comparatively show in Table 1. According to these results, T_{onset} increases in the order of $\text{VO}_x/\text{Al}_2\text{O}_3 > \text{VO}_x/\text{SP} > \text{VO}_x/\text{HT} > \text{VMgO}$, whereas T_{max} increases in the order of $\text{VO}_x/\text{Al}_2\text{O}_3 > \text{VO}_x/\text{SP} > \text{VO}_x/\text{HT} \sim \text{VMgO}$. Because the temperature at which the maximum hydrogen consumption is observed depends on the V loading and probably the dispersion, the reducibility of the catalyst can be better reflected by the onset temperature. On the other hand, a higher hydrogen consumption per V atom is observed on $\text{VO}_x/\text{Al}_2\text{O}_3$ (1.10 mol/V atom). It has been observed that the Al_2O_3 -supported vanadia catalyst presents an average oxidation state (AOS) after TPR experiments of 3.1, whereas the VMgO catalyst presents an AOS of 3.6.⁷ The results presented in Table 1 indicate that the main of the V ions in VO_x/SP and VO_x/HT present an AOS after the TPR experiments similar than that of the VMgO sample.

3.2. FTIR Spectroscopy. **3.2.1. IR Spectroscopy of Calcined and Reduced Catalyst.** Figure 1 shows the IR spectra in the low-frequency region (800–1200 cm^{-1}) of metal oxide supported vanadia catalysts before and after the reduction with hydrogen at 873 K. Overtones of vanadium species have not been detected in any case. No IR bands can be detected below 900 cm^{-1} because of the cutoff of the CaF_2 windows.

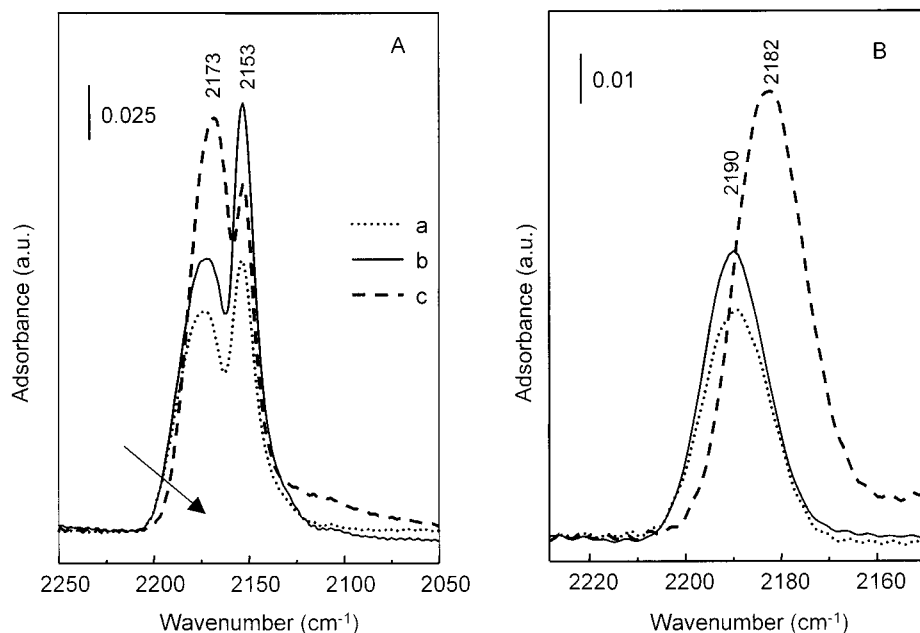


Figure 2. FTIR spectra of the VMgO sample after CO adsorption (20 hPa CO) at 85 K (A) and after subsequent evacuation at 85 K under dynamic vacuum for 1 min (B) of (a) sample calcined at 773 K, (b) sample reduced at 773 K, and (c) sample reduced at 873 K.

The IR spectrum of the calcined VMgO sample (Figure 1a) exhibits a band at 957 cm^{-1} . No change in the position of this band was observed after CO adsorption; however, this band is shifted to lower frequencies by increasing reduction temperature. Thus, the band at 957 cm^{-1} in calcined sample shifts to 933 cm^{-1} in the sample reduced at 773 K and to 923 cm^{-1} in the sample reduced at 873 K.

The IR spectrum of the calcined $\text{VO}_x/\text{Al}_2\text{O}_3$ sample exhibits two bands in the low-frequency region, at 1024 cm^{-1} and at 980 cm^{-1} (Figure 1b). As already reported in the literature, vanadium-oxo compounds give characteristic IR bands in the $800\text{--}1050\text{ cm}^{-1}$ region.^{40,41} Thus, the band at 1024 cm^{-1} can be assigned to the V=O stretching vibration of isolated vanadyl species ($\text{O}_3\text{V}=\text{O}$). The intensity of this band decreases with increasing reduction temperature, whereas the band at 980 cm^{-1} is slightly shifted to lower frequencies by reduction of the sample.

The IR spectrum of the calcined VO_x/HT sample (Figure 1c) exhibits a band at 971 cm^{-1} in the low-frequency region. This band remains unchanged after reduction at 773 K, but it is shifted to lower frequencies (923 cm^{-1}) after reduction at 873 K.

The IR spectra of the calcined VO_x/SP sample (Figure 1d) exhibits two bands at 1026 cm^{-1} (V=O stretching vibrations modes) and at 996 cm^{-1} . The intensity of the first band decreases slightly after reduction at 773 K and disappears after reduction of the sample at 873 K. The band at 996 cm^{-1} shifts to lower frequencies by increasing the reduction temperature and is observed at 975 cm^{-1} after reduction at 773 K and at 968 cm^{-1} after reduction at 873 K.

The bands at 957 cm^{-1} in VMgO, 980 cm^{-1} in $\text{VO}_x/\text{Al}_2\text{O}_3$, 996 cm^{-1} in VO_x/SP , and 971 cm^{-1} in VO_x/HT samples observed in the corresponding IR spectra have been commonly assigned to vanadium-oxo species. A band at 980 cm^{-1} is also observed on vanadium free Al_2O_3 catalyst. Therefore, we must indicate that these bands are not only related to vanadium species. In fact, assignment to the lattice vibrations or to the surface vibration modes could also be possible. On the other hand, the shifts in the position of these bands after reduction

treatments could be due to structural changes in the bulk of the catalysts. Thus, a phase transformation from magnesium orthovanadate, $\text{Mg}_3\text{V}_2\text{O}_8$, to the cubic spinel structure (MgV_2O_4) has been observed in the VMgO catalysts after treatment in reduction conditions.⁴²

3.2.2. IR Spectroscopy of CO Adsorbed at 85 K on Calcined and on Reduced Catalysts. VMGO. Adsorption of CO on the calcined sample leads to the appearance of two bands in the CO-stretching region at 2153 and 2173 cm^{-1} (Figure 2A, spectrum a). In parallel, the hydroxyl band at 3720 cm^{-1} (due to Mg-OH) observed on the calcined VMgO sample (spectra not shown) shifts to lower frequencies ($\Delta(\nu\text{OH}) = -31\text{ cm}^{-1}$) after adsorption of CO. By decreasing the CO adsorption pressure, the intensity of the band at 2153 cm^{-1} disappears together with a restoration of the original spectra of the OH groups. Thus, the band at 2153 cm^{-1} can be assigned to CO H-bonded to surface hydroxyl groups. However, the band at 2173 cm^{-1} still remains after complete elimination of CO interacting with OH groups. For this reason, this band can be assigned to CO coordinated to Lewis acid sites.

Similar spectra are obtained for VMgO samples reduced at 773 and 873 K (Figure 2A, spectra b and c, respectively), although the intensities of the bands change with the reduction temperature. In addition, the onset of the band centered at 2173 cm^{-1} is shifted to lower frequencies after reduction at 873 K.

The IR spectra in the CO stretching region recorded after CO evacuation at 85 K, on the calcined and reduced samples, are presented in Figure 2B. A band at 2190 cm^{-1} is observed for the calcined VMgO sample (Figure 2B, spectrum a). The stability of this band is low and is completely eliminated at increasing evacuation time. Because V^{4+} carbonyl compounds are expected to give bands between 2200 and 2180 cm^{-1} ,²⁵⁻²⁹ we infer that the band at 2190 cm^{-1} may be characteristic for V^{4+} -CO carbonyl species. This band is also observed on the reduced sample at 773 K (Figure 2B, spectrum b) confirming some stability with the reduction temperature.

Important differences can be observed, however, for the sample reduced at 873 K (Figure 2B, spectrum c), where an intense band at 2182 cm^{-1} is only observed. This band is very

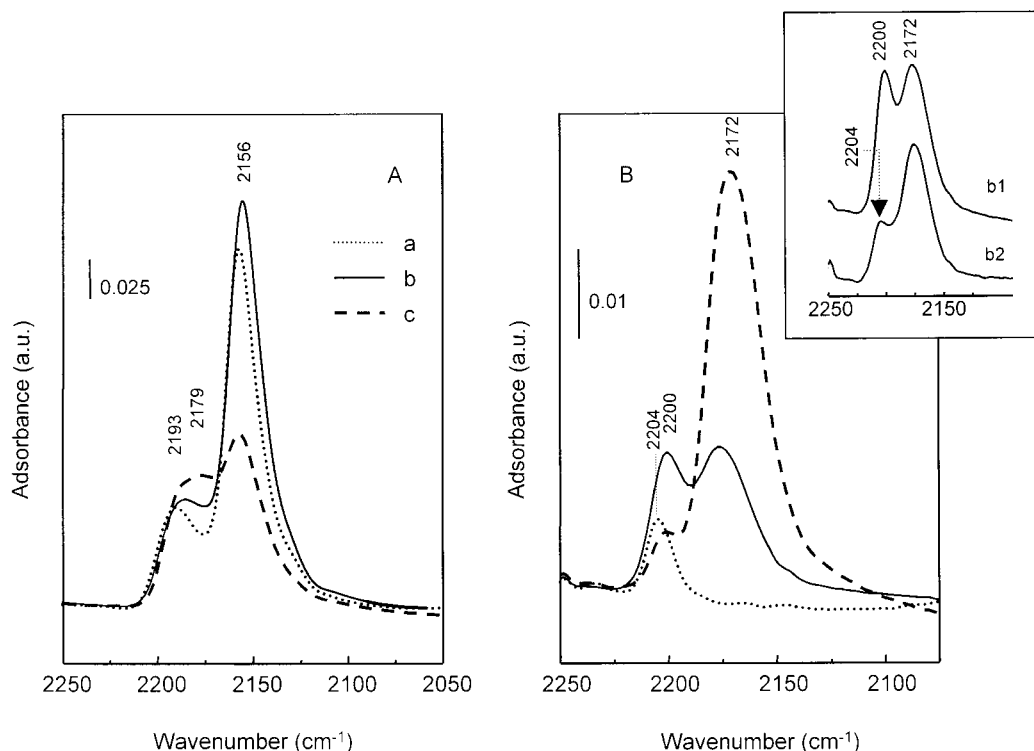


Figure 3. FTIR spectra of the $\text{VO}_x/\text{Al}_2\text{O}_3$ sample after CO adsorption (20 hPa CO) at 85 K (A) and after subsequent evacuation at 85 K under dynamic vacuum for 1 min (B) of (a) sample calcined at 773 K, (b) sample reduced at 773 K, and (c) sample reduced at 873 K. Inset: FTIR spectra of CO adsorption on the sample reduced at 773 K and at an evacuation time of 1 min (b1) and 2 min (b2). The spectra b1 and b2 are displaced for presentation.

stable even by increasing the temperature to 138 K under dynamic vacuum conditions. The high stability of this new band can be attributed to the formation of $\text{V}^{3+}\text{--CO}$ species.³⁶ In fact, the shift to lower frequencies of the onset of the band centered at 2173 cm^{-1} , after reduction at 873 K (see Figure 2A), might indicate a reduction of V^{4+} species to lower oxidation states. This is in agreement with recently reported data⁴² and with the results observed in the IR low-frequency region of this sample, in which in parallel to the reduction of V^{5+} to V^{3+} a phase transformation from magnesium orthovanadate to the cubic spinel structure (MgV_2O_4) is observed. According to these results, it can be concluded that $\text{Mg}_3\text{V}_2\text{O}_8/\text{Mg}_2\text{VO}_4/\text{MgV}_2\text{O}_4$ crystalline phases (with vanadium atoms in oxidation states +5, +4, and +3, respectively) could coexist during the reaction conditions when this catalyst is used in the oxidative dehydrogenation of short chain paraffins. The amount of each phase will depend on the alkane/oxygen ratio and/or alkane conversion level.

$\text{VO}_x/\text{Al}_2\text{O}_3$. Adsorption of CO on calcined $\text{VO}_x/\text{Al}_2\text{O}_3$ sample resulted in the appearance of two bands at 2156 (sharp band) and 2193 cm^{-1} (Figure 3A, spectrum a). The appearance of the band at 2156 cm^{-1} is parallel to a shift of the OH hydroxyl band to lower frequencies ($\Delta(\nu\text{OH}) = -85\text{ cm}^{-1}$). For this reason, the band at 2156 cm^{-1} can be related to CO adsorbed on the OH groups, whereas the band at 2193 cm^{-1} is due to CO interacting with Lewis acid sites.

Similar spectra have been observed on samples reduced at 773 and 873 K, with the appearance of new bands at 2188 and 2179 cm^{-1} , respectively.

The IR spectra in the CO stretching region recorded after CO evacuation on calcined and reduced samples are presented in Figure 3B (spectra a, b, and c). A band at 2204 cm^{-1} is only observed on the calcined sample (Figure 3B, spectrum a). This

band could be attributed to Al^{3+} Lewis acid sites (V-free sites on the surface of the support) or to $\text{V}^{4+}\text{--CO}$ species.

New bands at 2172 and 2200 cm^{-1} are observed on the sample reduced at 773 K (Figure 3B, spectrum b). In addition to these, a band at 2204 cm^{-1} is also observed at a high evacuation time (Figure 3B, spectrum b2). This band could be overlapped by the band at 2200 cm^{-1} in the spectrum obtained at low evacuation time (Figure 3B, spectrum b1).

The bands at 2172 and 2200 cm^{-1} are related to $\text{V}^{n+}\text{--CO}$ carbonyl compounds. The higher stability toward evacuation and the lower frequency of the band at 2172 cm^{-1} compared to that at 2200 cm^{-1} (Figure 3B, spectra b1 and b2) permits us to assign the former band to $\text{V}^{3+}\text{--CO}$ compounds and the latter one to $\text{V}^{4+}\text{--CO}$ species.³⁶

An increase of the intensity of the band at 2172 cm^{-1} is observed by increasing the reduction temperature to 873 K (Figure 3B, spectrum c). Thus, both V^{4+} and V^{3+} ions are observed in the $\text{VO}_x/\text{Al}_2\text{O}_3$ sample reduced at 773 K, whereas V^{4+} ions were only observed in the VMgO sample reduced at the same temperature. However, a quantitative analysis is not possible because of the unknown extinction coefficients of both $\text{V}^{n+}\text{--CO}$ carbonyl species.

On the other hand, the band at 2204 cm^{-1} is observed in the calcined sample (Figure 3B, spectrum a) or after high evacuation times in sample reduced at 773 (Figure 3B, spectrum b2) or 873 K (spectrum not shown). This band can be assigned to CO coordinated to Al^{3+} Lewis sites rather than to V^{n+} species.

VO_x/SP . Adsorption of CO on the calcined sample leads to the appearance of two bands at 2158 and 2177 cm^{-1} (Figure 4A, spectrum a). In parallel to the appearance of the band at 2158 cm^{-1} , the band of the OH hydroxyl bond shifts to lower frequencies ($\Delta(\nu\text{OH}) = -92\text{ cm}^{-1}$). For this reason, this band can be assigned to CO H-bonded to OH groups. On the other hand, the band at 2177 cm^{-1} , which behaves independent with

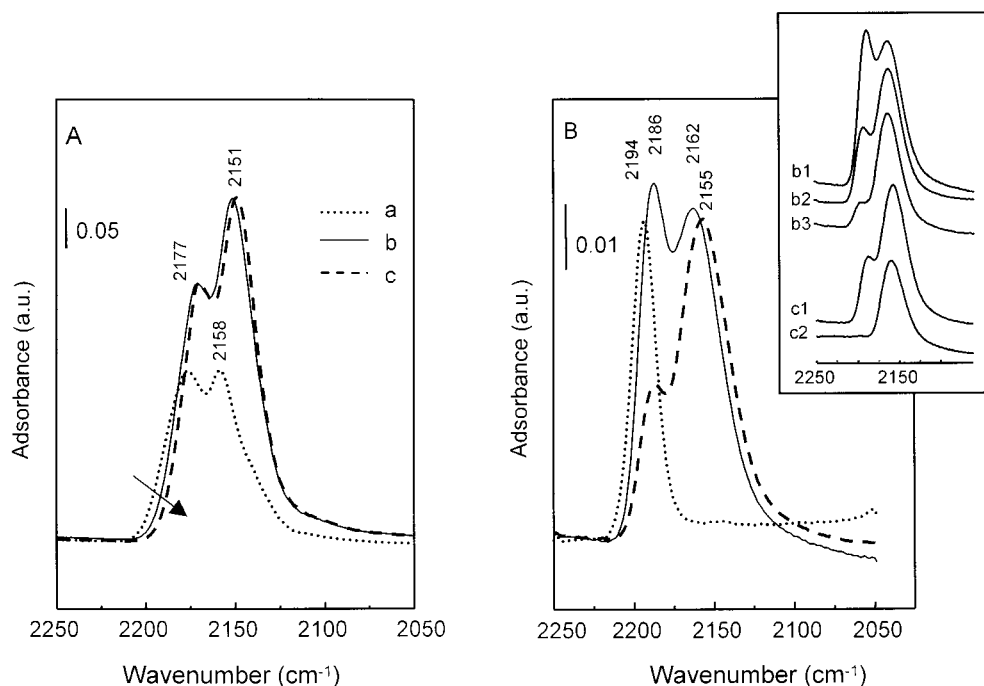


Figure 4. FTIR spectra of the VO_x/SP sample after CO adsorption (20 hPa CO) at 85 K (A) and after subsequent evacuation at 85 K under dynamic vacuum for 1 min (B) of (a) sample calcined at 773 K, (b) sample reduced at 773 K, and (c) sample reduced at 873 K. Inset: spectra b1, b2, and b3 have been obtained after evacuation times of 1, 3, and 5 min, respectively, whereas spectra c1 and c2 have been obtained after an evacuation time of 1 and 7 min, respectively. The spectra b1–b3 and c1–c2 are displaced for presentation.

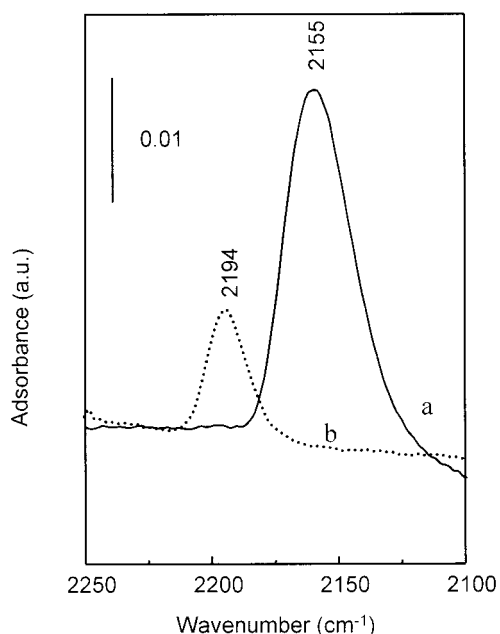


Figure 5. FTIR spectra of CO adsorbed on the VO_x/SP sample after reduction at 873 K during 1h (a) and after reoxidation with O_2 at 85 K (b). The spectra were recorded at 85 K under dynamic vacuum.

the shift of OH hydroxyl band, can be associated to CO interacting with Lewis acid sites as proposed for the VMgO sample. In addition to these bands, a shoulder can also be seen at 2140 cm^{-1} , which can be related to CO physically adsorbed on the calcined sample.

On the sample reduced at 773 K (Figure 4A, spectrum b), the OH–CO band is slightly shifted to lower values (2151 cm^{-1}). The poor signal-to-noise ratio of the spectra in the OH region made the observation of any spectral change of the hydroxyl groups impossible. Small changes have been observed in the carbonyl IR spectra of adsorbed CO at 85 K on the sample

reduced at 873 K (Figure 4A, spectrum c). The gradual shift of the onset of the band centered at 2177 cm^{-1} to lower frequencies at increasing reduction temperature accounts for a reduction of the vanadium species to lower oxidation states.

The IR spectra in the CO stretching region recorded after CO evacuation at 85 K on calcined, reduced, and reoxidized samples are compared in Figure 4B. A single band at 2194 cm^{-1} (Figure 4B, spectrum a) is observed on calcined samples. This band remains stable after prolonged evacuation of the sample and can therefore be attributed either to Al^{3+} acid sites of the support (with lower acidity than pure Al_2O_3 as a consequence of the presence of Mg^{2+} ions in the spinel) or to V^{4+} –CO species. In this case, V^{4+} species would have to be formed during evacuation of the oxidized sample at 10^{-3} Pa and 773 K prior to the CO adsorption experiment.

The IR spectrum of the sample reduced at 773 K shows two bands centered at 2162 and 2186 cm^{-1} (Figure 4B, spectrum b). The relative intensities of these bands change with the evacuation time, whereas a band at 2194 cm^{-1} is also observed at increasing evacuation time (Figure 4B, spectra b1–b3). According to this, the stability of these bands decreases in the order of $2162 \gg 2194 > 2186\text{ cm}^{-1}$. On the other hand, considering the frequency position and the stability of these bands, the band at 2162 cm^{-1} can be assigned to V^{3+} –CO species. On the other hand, the bands at 2186 and 2194 cm^{-1} can be related to two different kinds of V^{4+} species or to V^{4+} ions (band at 2186 cm^{-1}) and Al^{3+} ions (band at 2194 cm^{-1}), respectively.

On the sample reduced at 873 K (Figure 4B, spectrum c), a new band at 2155 cm^{-1} , together with the band at 2186 cm^{-1} , is observed. In this case, no band at 2194 cm^{-1} is observed. The stability of the band at 2155 cm^{-1} is significantly higher than that of the band at 2186 cm^{-1} (Figure 4B, spectra c1–c2), which indicates the formation of V^{n+} –CO carbonyl species in an oxidation state lower than 4. Note that the band at 2155 cm^{-1} appears at a slightly lower frequency than the band at 2162

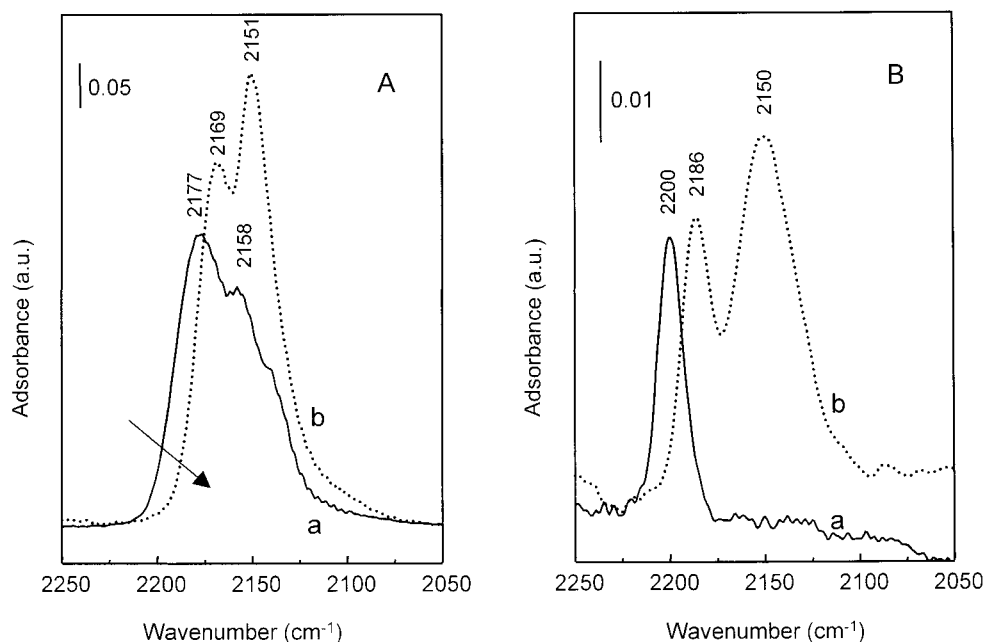


Figure 6. FTIR spectra of the VO_x/HT sample after CO adsorption (25 hPa CO) at 85 K (A) and after subsequent evacuation at 85 K under dynamic vacuum for 1 min (B) of (a) sample reduced at 773 K and (b) sample reduced at 873 K.

cm⁻¹ (observed on the sample reduced at 773 K). Both bands are highly stable toward evacuation. Because polyvanadate species have been proposed to be present on this sample,^{6,43} we can infer the band at 2155 cm⁻¹ to be related to the V³⁺—O—V³⁺ species (formed at higher reduction temperature), whereas the band at 2162 cm⁻¹ might be related to the V⁴⁺—O—V³⁺ species (formed at lower reduction temperature). Such changes in the near coordination sphere of the V³⁺ species may explain changes in the frequencies of the V³⁺—CO carbonyl species. However, the possible formation of V²⁺ ions cannot be excluded.

Reoxidation experiments at low temperature have been done in order to study the nature of reduced vanadium ions related to the band at 2155 cm⁻¹ observed in the reduced sample. Figure 5 shows the IR spectra of the sample reoxidized at 85 K. The band observed in the reduced sample at 2155 cm⁻¹ disappears completely, whereas a new band at 2194 cm⁻¹ is observed after reoxidation. The reappearance of the band at 2194 cm⁻¹ (also present on calcined samples and samples reduced at 773 K) after reoxidation at 85 K indicates that this band is due to vanadium species rather than to Al³⁺ ions. Thus, it can be concluded that the reduced vanadium species in the VO_x/SP sample presents high reoxidation ability.

VO_x/HT. The IR spectra of CO adsorption on a VO_x/HT sample reduced at 773 and 873 K are shown in Figure 6A. Two broad and overlapping bands at 2158 (due to CO adsorbed on OH groups) and 2177 cm⁻¹ (due to CO interacting with Lewis acid sites) are observed after CO adsorption on the sample reduced at 773 K (Figure 6A, spectrum a). We must indicate that the appearance of the band at 2158 cm⁻¹ is parallel to a shift of the band of OH hydroxyl bond to lower frequencies ($\Delta(\nu_{\text{OH}}) = -59$ cm⁻¹).

On the sample reduced at 873 K, only two bands at 2151 (CO H-bonded with OH groups) and 2169 cm⁻¹ (CO interacting with Lewis acid sites; Figure 6A, spectrum b) are observed. On the other hand, the onset of the band centered at 2177 cm⁻¹ in the sample reduced at 773 K is shifted to lower frequencies when the reduction temperature increases to 873 K. This could be due to a progressive reduction of the V⁴⁺ species to lower oxidation states.

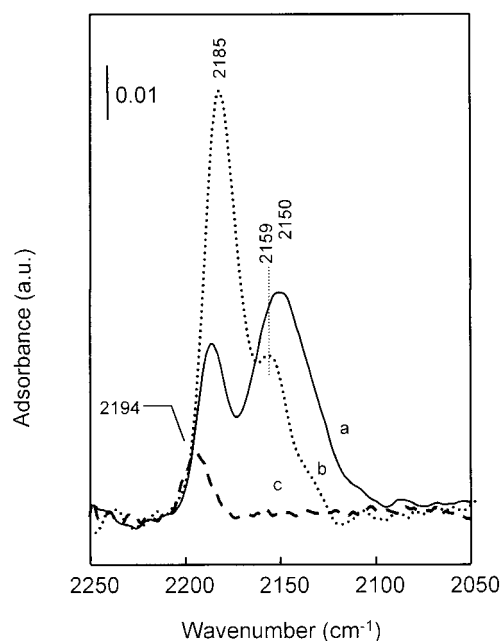


Figure 7. FTIR spectra of VO_x/HT sample (a) reduced at 873 K, (b) reoxidized with O₂ at 85 K, and (c) reoxidized with O₂ at 298 K.

The IR spectra in the CO stretching region recorded after CO evacuation on reduced sample are presented in Figure 6B. A band at 2200 cm⁻¹ is only observed on the sample reduced at 773 K, which can tentatively be assigned to V⁴⁺ ions (Figure 6B, spectrum a). However, this band disappears, and new bands at 2150 and 2186 cm⁻¹ are observed in the spectrum of the sample reduced at 873 K (Figure 6B, spectrum b).

Reoxidation experiments have also been performed in order to study the nature of the vanadium species associated to the bands at 2150 and 2186 cm⁻¹ in reduced sample. Figure 7 shows the IR spectra of the reoxidized samples. The band at 2150 cm⁻¹ (observed in reduced sample) disappears, whereas the intensity of the band at 2185 cm⁻¹ increases when the sample is reoxidized at 85 K (Figure 7, spectrum b). In addition, a new band at 2159 cm⁻¹ is also observed. According to these results,

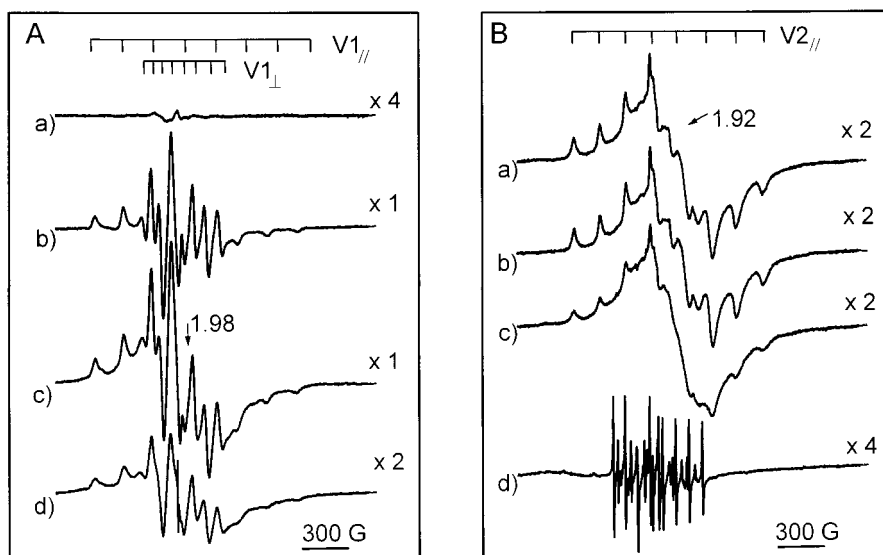


Figure 8. EPR spectra of $\text{VO}_x/\text{Al}_2\text{O}_3$ (A) and VMgO (B) samples after calcination at 773 K (a) and reduced at 573 (b), 673 (c), and 873 K (d).

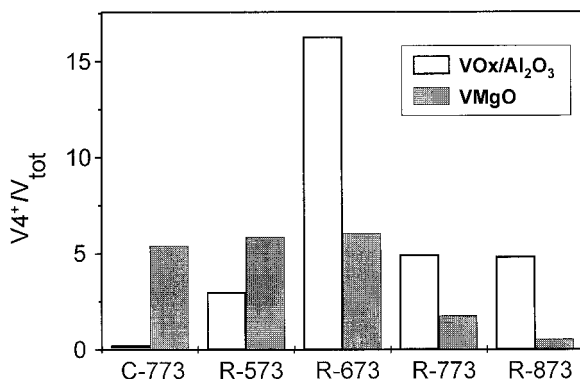


Figure 9. Relative abundance of V^{4+} ions in the $\text{VO}_x/\text{Al}_2\text{O}_3$ and VMgO samples after calcination in air at 773 K (C-773) and after reduction at 573 (R-573), 673 (R-673), 773 (R-773), and 873 K (R-873).

the band at 2150 cm^{-1} , associated to easily reoxidized V species, can be assigned to V^{3+} . However, the presence of V^{2+} species in the reduced sample cannot be completely ruled out.²⁸

After reoxidation at 298 K, a band at 2194 cm^{-1} is observed, whereas the bands at 2186 and 2159 cm^{-1} (observed in the sample reoxidized at 85 K) disappear completely (Figure 7, spectrum c). These bands are easily oxidized at a higher temperature (298 K), whereas other V^{4+} species, characterized by the band at 2194 cm^{-1} , remain on the oxidized sample at 298 K. So, these bands could be assigned to two V^{4+} species with different redox properties.

3.3. EPR Spectroscopy. EPR spectroscopy of supported vanadium catalysts, $\text{VO}_x/\text{Al}_2\text{O}_3$ and VMgO , were carried out in order to study the influence of the acid–base character of the support on the redox behavior of the vanadium species. Figure 8 shows the EPR spectra of $\text{VO}_x/\text{Al}_2\text{O}_3$ and VMgO samples in the initial calcined state and after reduction in H_2 at reduction temperatures (T_r) between 573 and 873 K. On the other hand, Figure 9 presents the relative abundance of the V^{4+} species in these experiments relative to the total number of V atoms in the samples.

A very weak ill-defined signal is observed for calcined $\text{VO}_x/\text{Al}_2\text{O}_3$ sample (Figure 8A, spectrum a). Reduction in H_2 leads to the appearance of different V^{4+} signals (Figure 8A, spectra b–d), with a maximum of the relative abundance of V^{4+} at $T_r = 673\text{ K}$ (Figure 9). The spectra observed can be rationalized by considering the presence of two overlapping signals. An axial

signal V1 shows a hyperfine structure of eight lines in each of its components arising from magnetic interaction of the unpaired electron with the ^{51}V nucleus ($I = 7/2$, natural abundance 99.75%), and with parameters $g_{\perp} = 1.975$, $A_{\perp} = 6.3 \times 10^{-3}\text{ cm}^{-1}$, $g_{\parallel} = 1.933$, and $A_{\parallel} = 17.7 \times 10^{-3}\text{ cm}^{-1}$. A broad ($\Delta H_{\text{pp}} \approx 160\text{ G}$) featureless symmetric signal VV with $g \approx 1.98$ is also evident from the baseline distortion in the hyperfine features of signal V1 in some of the spectra.

The well resolved hyperfine structure and the EPR parameters of signal V1 are consistent with its attribution to VO^{2+} species in a square pyramidal or distorted octahedral environment.⁴⁴ The g value of the broad signal VV and the absence of hyperfine structure indicate that it is due to magnetically interacting V^{4+} sites.^{45,46}

Analysis of the spectra of $\text{VO}_x/\text{Al}_2\text{O}_3$ evidences the higher reducibility of isolated vanadium sites giving rise to the VO^{2+} signal V1 because it appears already for $T_r = 573\text{ K}$. However, the reduction of the more interacting vanadium sites (broad signal VV) does not become apparent until $T_r = 673\text{ K}$. Both entities show maximum intensity at $T_r = 673\text{ K}$ suggesting further evolution of the reduction process, leading to V^{3+} species for higher T_r .

The EPR spectra observed for calcined VMgO or for the sample reduced at $T_r = 573$ – 673 K are mainly constituted of two overlapping signals (Figure 8B). The first signal, V2, showing resolved hyperfine features in the parallel component at $g_{\parallel} = 1.942$ and $A_{\parallel} = 15.0 \times 10^{-3}\text{ cm}^{-1}$, can be attributed to isolated VO^{2+} species in a square pyramidal or distorted octahedral environment⁴⁴ as in the case of signal V1. The differences between both signals can be ascribed to variations in the local environment of the centers in the two samples. The second signal, which is predominant in the spectra, is similar to signal VV although it shows a lower g value ($g \approx 1.92$). These differences suggest that the corresponding V^{4+} centers might also be affected by interactions with the support. In contrast to sample $\text{VO}_x/\text{Al}_2\text{O}_3$, an appreciable amount of V^{4+} is detected already for the calcined sample (Figure 9), and strong changes in the relative abundance of total V^{4+} are not detected during the reduction process up to $T_r = 673\text{ K}$. This can be explained by a compensating effect involving an increase of signal VV and a decrease of signal V2 for $T_r = 673\text{ K}$. This latter observation evidences the higher reducibility of isolated vanadium sites in VMgO . A significant decrease of the relative

abundance of V^{4+} sites is produced for $T_r > 673$ K (Figure 9), suggesting the generation of V^{3+} species at $T_r > 673$ K as in the case of sample VO_x/Al_2O_3 . Only weak narrow signals corresponding to isolated VO^{2+} species (and a very weak signal that is due to Mn^{2+} impurities) are observed in the spectrum of VMgO reduced at $T_r = 873$ K, indicating the higher reducibility of vanadium oxide entities in this sample.

4. Discussion

According to previously reported NMR results,^{6,43} tetrahedral V^{5+} species are the major vanadium species in all of the catalysts studied, although the dispersion degree of the vanadium species depends on the acid–base character of the metal support. Thus, isolated VO_4 tetrahedra are mainly observed on the basic oxide supports (MgO and calcined hydrotalcite), whereas pyrovanadate and metavanadate type species are predominantly observed on the more acidic metal oxide supports (Al_2O_3 and Mg/Al–spinel).

The redox properties of the vanadium oxide surface compounds depend also on the acid–base nature of the catalyst support. Hence, TPR experiments show that the reducibility of the vanadium species supported on the more acidic supports (Al_2O_3 and Al/Mg–spinel) is higher than those supported on MgO and hydrotalcite (see Table 1).⁶ Supporting results were obtained from both IR spectra of CO adsorption at 85 K and EPR results. V^{5+} species are mainly present on the calcined samples. However a small amount of V^{4+} was also observed in some cases as a consequence of a partial reduction of the catalysts during evacuation pretreatment at high temperature prior to CO adsorption. In the case of the VMgO sample, the presence of V^{4+} species in calcined sample can be related to the formation of V–Mg–O solid compounds.⁴⁷ These V–Mg–O solid compounds are also observed on other Mg-containing catalysts such as VO_x/HT or $VO_x/sepiolite$.^{1,7,38}

The carbonyl IR spectra of reduced samples suggest the presence of V^{4+} ions together with V^{3+} ions on VO_x/Al_2O_3 samples reduced at 773 and 873 K. Because the TPR (Table 1) and IR results indicate a similarity between VO_x/Al_2O_3 and VO_x/SP catalysts, it can be concluded that the reduction of V^{5+} to the V^{3+} species seems to be more favored on acidic supports (VO_x/Al_2O_3 and VO_x/SP catalysts).

In the case of the VMgO sample, V^{4+} ions are only observed on the sample reduced at 773 K, whereas V^{3+} ions were observed in the sample reduced at 873 K. On the other hand, both TPR and IR results indicate a similarity in the redox properties of VMgO and VO_x/HT catalysts. So, the reducibility on catalysts supported on basic supports seems to be hindered, leading to the formation of V^{4+} species. V^{3+} ions are also formed on basic supports, but they are formed at high reduction temperatures. The lower reducibility of V species on a basic support could be related to the formation of a most stable VO_x –MgO solid compound.

V^{4+} species have also been observed by EPR spectroscopy of reduced VMgO and VO_x/Al_2O_3 samples, although the nature and the amount of the V^{4+} species depends on the metal oxide support and reduction temperature (Figure 8). Thus, an axial signal related to VO^{2+} species in a square pyramidal or distorted octahedral environment was mainly observed on VO_x/Al_2O_3 reduced at 673 K. However, a broad symmetric signal VV with $g \approx 1.92$ is mainly observed on VMgO reduced at 673 K.

The intensities of these signals of V^{4+} species observed by EPR decrease at reduction temperatures higher than 673 K, although the disappearance of the V^{4+} species on reduced VO_x/Al_2O_3 sample occurs more quickly than that on the VMgO sample (Figure 9). This is in agreement with the lower

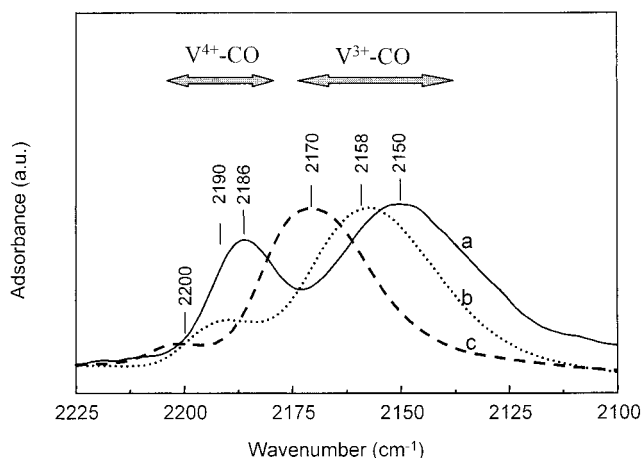


Figure 10. FTIR spectra of the CO stretching vibration after adsorption on (a) VO_x/HT , (b) VO_x/SP , and (c) VO_x/Al_2O_3 samples reduced at 873 K. The spectra were recorded at 85 K under dynamic vacuum.

reducibility of the VMgO sample observed by IR spectra of CO, in which the presence of V^{3+} species was only observed at high reduction temperatures (873 K).

An influence of the acid–base properties of the catalyst supports on the nature and properties of the reduced vanadium species can be considered. In fact, the carbonyl stretching frequency of the V^{4+} –CO and V^{3+} –CO complexes are shifted to lower frequencies by increasing basicity of the support, as suggested by the spectra shown in Figure 10. This trend could be explained by the electronic effects of the support on the properties of the vanadium ions. Basic supports may act as electron donor ligands, whereas acidic supports may act as electron acceptor ligands. Thus, a higher basicity of the support would increase the electron density at the vanadium ions. This leads to a higher π -bonding ability of the V^{3+} ions and, consequently, to a weakening of the C–O bonds which results in a shift of the carbonyl stretching frequency to lower frequencies. In addition, higher support basicity would also lead to a lower acid strength of the V^{4+} ions, thus reducing the V^{4+} ← CO σ -donor bond strength which leads to a C–O stretching frequency closer to the gas phase. In the case of the VMgO catalyst, this trend is not observed probably because of the formation of a solid solution of the vanadium species with different oxidation states in the MgO support. $Mg_3V_2O_8$ coexists with Mg_2VO_4 (V^{4+}) and/or MgV_2O_4 (V^{3+}) in VMgO samples without changes in the crystal structure of the catalyst as it has been suggested recently.⁴²

On the other hand, IR results of CO adsorbed (at 85 K) on reoxidized VO_x/HT and VO_x/SP samples indicate a different reoxidation rate of reduced V species. V^{4+} and V^{3+} species were observed on a reduced VO_x/SP sample, but they were easily oxidized at 85 K. However, V species in a reduced VO_x/HT sample were only partially reoxidized at 85 K, although total reoxidation was achieved at 298 K. These results are in agreement with those observed for VMgO and Al_2O_3 supported vanadium catalyst. In fact, the reoxidation rate of a VO_x/Al_2O_3 catalyst was about 10 times higher than that of a VMgO catalyst.¹² Thus, one may expect that the reoxidation rate of vanadium species in V/HT and V/SP samples should be intermediate between those obtained in VMgO and VO_x/Al_2O_3 catalysts.

Finally, the results presented here may help us to understand the catalytic behavior of these catalysts in the oxidative dehydrogenation of C_2 – C_5 alkanes. The catalytic activity of these materials appears to be related to the reducibility of the

vanadium species ($\text{VO}_x/\text{Al}_2\text{O}_3 > \text{VO}_x/\text{SP} > \text{VMgO} > \text{VO}_x/\text{HT}$). However, the selectivity to OXDH products is related to both the acid–base character of the catalysts and the alkane feed.^{1,6,7} Thus, the selectivity to oxydehydrogenation products decreases in the trend: $\text{VMgO} > \text{VO}_x/\text{HT} > \text{VO}_x/\text{SP} > \text{VO}_x/\text{Al}_2\text{O}_3$ (during the OXDH of *n*-butane to C_4 -olefins) or $\text{VO}_x/\text{Al}_2\text{O}_3 > \text{VO}_x/\text{SP} > \text{VO}_x/\text{HT} > \text{VMgO}$ (during the OXDH of ethane to ethylene).

5. Conclusions

Tetrahedral V^{5+} species are mainly present on our catalysts, although the aggregation of V^{5+} species increases with the acid character of the oxide support. TPR results of supported vanadia catalysts indicated that the reducibility of vanadium species supported on basic oxide supports is lower than that on acidic oxide supports.

IR study of the adsorption of CO on calcined and reduced supported vanadia catalysts were carried out in order to elucidate the nature of V species after the reduction in hydrogen. No carbonyl species were formed in calcined samples, suggesting that V^{5+} are only present on the surface of the catalysts. However, $\text{V}^{4+}\text{--CO}$ and $\text{V}^{3+}\text{--CO}$ carbonyl species were observed in reduced samples.

The IR spectra of CO adsorbed on reduced samples indicate that the reduction of V species in basic oxide supports leads to the formation of V^{4+} species at 773 K. However, the higher reducibility observed for vanadia supported on acidic oxide supports leads to the formation of both V^{4+} and V^{3+} species at the same reduction temperature. This is confirmed by the TPR and EPR results in which the higher reducibility corresponds to vanadium species supported on alumina.

On the other hand, it has been observed that the carbonyl frequencies of the $\text{V}^{4+}\text{--CO}$ and $\text{V}^{3+}\text{--CO}$ complexes are shifted to lower frequencies with increasing basicity of the support. This can be explained by an effect of the support on the electron density of the vanadium species. In addition, a higher reoxidation ability of the V^{4+} and V^{3+} species is observed on the more acidic supports (VO_x/SP) than on the basic ones (VO_x/HT).

It was previously observed that the catalytic behavior in the oxidative dehydrogenation of these catalysts depends on both the redox and acid–base character.^{6,7} According to our results, different oxidation states of the vanadium species depending on the acid–base character of the metal oxide support can be monitored by means of IR spectroscopy of adsorbed CO. On the other hand, information on the electrophilic character of the vanadium species, related to the acid–base character of the metal oxide support, can be obtained. The modification of the electrophilic character can influence the redox properties of the vanadium species, which determine the catalytic activity of these catalysts during the oxidative dehydrogenation of alkanes.

Acknowledgment. The work done in Munich was financially supported by the Deutsche Forschungsgemeinschaft (SFB 338) and by the Funds der Chemischen Industrie. P.C. acknowledges a grant from the Funds der Chemischen Industrie. The Spanish authors are grateful for the financial contribution by Comisión Interministerial de Ciencia y Tecnología, CICYT (Project PPQ 2000-1396). The permission of Prof. J. Soria (ICP, Spain) to the use of the EPR Spectrometer is gratefully acknowledged.

References and Notes

- Blasco, T.; López Nieto, J. M. *Appl. Catal. A: General* **1997**, *157*, 117.
- Albonetti, S.; Cavani, F.; Trifiró, F. *Catal. Rev. Sci. Eng.* **1996**, *38*, 413.
- Centi, G. *Appl. Catal. A: General* **1996**, *147*, 267.
- Deo, G.; Wachs, I. E.; Haber, J. *Crit. Rev. Surf. Chem.* **1994**, *4*, 141.
- Bond, G. C.; Tahir, S. F. *Appl. Catal.* **1991**, *71*, 1.
- Blasco, T.; López Nieto, J. M.; Dejoz, A.; Vázquez, M. I. *J. Catal.* **1995**, *157*, 271.
- López Nieto, J. M.; Concepción, P.; Dejoz, A.; Knözinger, H.; Melo, F.; Vázquez, M. I. *J. Catal.* **2000**, *189*, 147.
- Bars, Le; Vedrine, J.; Auroux, J. C.; Trautmann, A.; Baers, M. *Appl. Catal.* **1992**, *88*, 179.
- Eon, J. G.; Olier, R.; Volta, J. C. *J. Catal.* **1994**, *145*, 318.
- Kung, H. H.; Chaar, M. A. U.S. Patent 4,772,319, 1988.
- Deo, G.; Wachs, I. E. *J. Phys. Chem.* **1991**, *95*, 5889.
- López Nieto, J. M.; Soler, J.; Concepción, P.; Herguido, J.; Menéndez, M.; Santamaría, J. *J. Catal.* **1999**, *185*, 324.
- Hadjiivanov, K.; Lamotte, J.; Lavalley, J. C. *Langmuir* **1997**, *13*, 3374.
- Zaki, M. I.; Knözinger, H. *Spectrochim. Acta* **1987**, *43A*, 1455.
- Neyman, K. M.; Strodel, P.; Ruzankin, S. Ph.; Schlensog, N.; Knözinger, H.; Rösch, N. *Catal. Lett.* **1995**, *31*, 273.
- Knözinger, H. In *Proceedings of the International Symposium On Acid–Base Catalysis*; Tanabe, K., Hattori, H., Yamaguchi, T., Tanaka, T., Eds.; Kodansha: Tokyo, 1989; p 147.
- Strodel, P.; Neyman, K. M.; Knözinger, H.; Rösch, N. *Chem. Phys. Lett.* **1995**, *240*, 547.
- Hadjiivanov, K.; Lavalley, J. C.; Lamotte, J.; Maugé, F.; Saint-Just, J.; Che, M. *J. Catal.* **1998**, *176*, 415.
- Hadjiivanov, K.; Kantcheva, M. M.; Klissurski, D. G. *J. Chem. Soc., Faraday Trans.* **1996**, *92*, 4595.
- Hush, N. S.; Williams, M. L. *J. Mol. Spectrosc.* **1974**, *50*, 349.
- Larsson, R.; Lykvist, R.; Rebenstorf, B. *Z. Phys. Chem (Leipzig)* **1982**, *263*, 1089.
- Zaki, M. I.; Vielhaber, B.; Knözinger, H. *J. Phys. Chem.* **1986**, *90*, 3176.
- Harrison, P. G.; Thornton, E. W. *J. Chem. Soc., Faraday Trans. 1* **1978**, *74*, 2703.
- Hadjiivanov, K.; Klissurski, D.; Davydov, A. *J. Chem. Soc., Faraday Trans. 1* **1988**, *84*, 37.
- Sobalic, Z.; Kozłowski, R.; Haber, J. *J. Catal.* **1991**, *127*, 665.
- Gerasimov, S.; Filimonov, V. *Kinet. Catal.* **1981**, *22*, 469.
- Jonson, B.; Rebenstorf, B.; Larsson, R.; Andersson, S. L. T. *J. Chem. Soc., Faraday Trans. 1* **1988**, *84*, 1897.
- Jonson, B.; Rebenstorf, B.; Larsson, R. *Acta Chem. Scand.* **1988**, *A42*, 156.
- Davydov, A. *IR Spectroscopy of Adsorbed Species on the Surface of Transition Metal Oxides*; C. H. Ed.; John Wiley & Son: New York, 1990.
- Jonson, B.; Rebenstorf, B.; Larsson, R.; Andersson, S. L. T. *J. Chem. Soc., Faraday Trans. 1* **1988**, *84*, 3363.
- Davydov, A.; Budneva, A.; Maksimov, N. G. *React. Kinet. Catal. Lett.* **1982**, *20*, 93.
- Davydov, A.; Shepotko, M. *Teor. Ekspn. Khim.* **1990**, *26*, 505.
- Maschenko, A.; Kou, M.; Shvets, V.; Kazanskii, V. *Teor. Eksp. Khim.* **1972**, *8*, 801.
- Busca, G.; Ramis, G.; Lorenzelli, V. *J. Mol. Catal.* **1989**, *50*, 231.
- Concepción, P.; Reddy, B. M.; Knözinger, H. *Phys. Chem. Chem. Phys.* **1999**, *1*, 3031.
- Concepción, P.; Hadjiivanov, K.; Knözinger, H. *J. Catal.* **1999**, *184*, 172.
- Corma, A.; López Nieto, J. M.; Paredes, N. *J. Catal.* **1993**, *144*, 425.
- López Nieto, J. M.; Dejoz, A.; Vázquez, M. I. *Appl. Catal. A: General* **1995**, *132*, 41.
- Kunzmann, G. Ph.D. Thesis, Universität München, 1987.
- Gao, X.; Ruiz, P.; Xin, Q.; Guo, X.; Delmon, B. *J. Catal.* **1994**, *148*, 56.
- Siew Hew Sam, D.; Soenen, V.; Volta, J. C. *J. Catal.* **1990**, *123*, 417.
- Burrows, A.; Kiely, C. J.; Perregaard, J.; Højlund-Nielsen, P. E.; Vorbeck, G.; Calvino, J. J.; López-Cartes, C. *Catal. Lett.* **1999**, *57*, 121.
- Blasco, T.; López Nieto, J. M. *Colloids Surf. A* **1996**, *115*, 187.
- Prakash, A. M.; Kevan, L. *J. Phys. Chem. B* **1999**, *103*, 2214.
- Blasco, T.; Concepción, P.; López Nieto, J. M.; Martínez-Arias, A.; *Proceedings of the 12th International Zeolite Conference*; Treacy, M. M. J., Markus, B. K., Bisher, M. E., Higgins, J. B., Eds.; Materials Research Society: Warrendale, PA, 1999; p 2473.
- Lapina, O. B.; Shubin, A. A.; Nosov, A. V.; Bosh, E.; Spengler, J.; Knözinger, H. *J. Phys. Chem. B* **1999**, *103*, 7599.
- Corma, A.; López Nieto, J. M.; Paredes, N. *Appl. Catal. A: General* **1993**, *104*, 161.